

Determination of Frequency Dependent Fluid Damping of Micro and Nano Resonators for Different Cross-Sections

Weibin Zhang, Michael Requa, Kimberly Turner
 Mechanical Engineering, University of California at Santa Barbara
 Santa Barbara, CA 93106-5070
 {weibin,requa,turner}@engineering.ucsb.edu

ABSTRACT

This research quantitatively investigates fluid damping of MEMS and NEMS flexural resonators such as scanning probe and carbon nano-tube resonators, aiming to improve the quality factor prediction and therefore the resonator design. Fluid damping in beam-type resonators is most affected by resonant frequency, device dimensions and cross-sectional shape which are systematically examined within. An experimentally motivated linear fluid damping model is rendered with numerical methods and a general fluid damping law is achieved with limited error. By generalizing to include rectangular, circular and trapezoidal cross-sections, this analysis encompasses a cadre of micro- and nano- scale beam resonators including cantilevers, carbon nanotubes and scanning probe, respectively.

Keywords: resonator, quality factor, fluid damping, drag force, resonant frequency

1 INTRODUCTION

Quality factor (Q) is one of the key parameters for Micro(or Nano)-Electro-Mechanical (MEM or NEM) resonators, affecting the resonant amplitude, bandwidth, sensitivity and etc [1]. Most micro- and nano- scale resonators require a vacuum operating condition to achieve a high Q factor. There are also many applications requiring “in-fluid” sensing and actuation, in which case the resonators operate in high damping conditions such as air and liquid [2]. For example, in [3], the authors demonstrate a parametric resonance based mass sensor which shows good sensitivity when operated in air. Also many scanning probe microscope (SPM) measurements take place in air or liquid conditions. This work offers design tools for beam type resonators which necessitate operation in environments where fluid damping caused by the drag force is the dominant damping source.

In this work it is assumed that the flexural resonators oscillate in an infinite fluid with small amplitude, whereby the flow can be simplified as a two-dimensional problem in the cross-sectional plane of the resonator. Other damping mechanisms such as so-called “squeeze-film” damping are not considered. By this assumption there are three factors which significantly affect the fluid damping, namely resonant frequency, device dimensions and the cross-sectional shape.

Table 1: Nomenclature

μ	Viscosity of the fluid
ρ	Density of the fluid
u	Velocity of the resonator
F	Fluid drag force per unit length
ω	Resonant frequency
δ	Penetration depth defined in ??
$C_{damping}$	Damping coefficient = $\frac{F}{u}$
λ	Defined in (2)
γ	Euler’s constant (≈ 0.577)
Re	Reynolds number defined as $\frac{\rho u d_2}{\mu}$
(a, b)	Dimensionless coefficients in (1)
d_1, d_2	Show in figure 4, $d_1 \parallel u, d_2 \perp u$

High resonant frequency is a key advantage of MEMS and NEMS resonators for certain applications [4]. But for the high frequency “in-fluid” oscillation, the fluid damping characteristics behave dramatically different compared to the low frequency or the steady flow cases. This results in frequency-dependent fluid damping. On the other hand, the cross-sectional dimensions, especially the dimensions perpendicular to the flow (in this example, it is the width of the cantilever), play an important role in the fluid damping. Cross-sectional shape of the device is also an influential factor, as we will show, at least for the steady flow [5]. Resonators with three kinds of cross-section shapes are considered: cantilever with rectangular cross-section, carbon nanotube with circular cross-section, and scanning probe with trapezoid cross-section.

In [6], by studying the pressure dependant damping of MEMS cantilevers for different resonant modes, a new linear fluid damping model was empirically proposed:

$$C_{damping} = (a + b\lambda)\pi\mu \quad (1)$$

where $C_{damping}$ is the damping coefficient, (a, b) is the cross-section shape dependent constant pair and λ is a dimensionless parameter defined as the ratio of the width of cantilever to the so-called penetration depth (δ) of the viscous fluid.

$$\lambda = \frac{\text{Width}}{\delta}, \quad \delta = \sqrt{\frac{2\mu}{\rho\omega}} \quad (2)$$

Model (1) is based on the experimental observations for MEMS cantilevers with rectangular cross-section shape. A

parameter pair (a, b) was determined for cantilevers with fixed thickness [6]. In this paper, we generalize (1) to flexural resonators with different cross-sections to find a more universal law to describe the fluid damping. To achieve this, the following questions need consideration.

- Is model (1) applicable to other types of flexural resonators?
- For different types of cross-section, how to determine the parameters a and b ?
- How much is the overall error using (1)?

As stated above, model (1) is based on experimental observations, but in this paper, we emphasize numerical analysis. Numerical simulation opens another door to understand the fluid damping physics, not only can it be used to validate model (1), it also help to generalize the model.

The paper is organized in the following way: First we introduce the numerical procedure and compare the results to experiments. Then we determine parameters a and b individually and investigate their dependence on differently shaped cross-sections. By doing so, we generalize the damping model, and the overall error will be discussed.

2 NUMERICAL SIMULATION

Compared to the experiment, numerical simulation provides a relatively “cheap” way to explore the influence of various and irregular cross-section shapes on fluid damping.

2.1 Procedure

The finite element analysis software COMSOL was used for the numerical modeling. The software provided the ability to deal with moving boundary problem using the Arbitrary-Lagrangian-Eulerian (ALE) algorithm. Basically the procedure to find the fluid drag force contains three steps:

- solve the moving boundary problem
- solve the incompressible Navier-Stokes flow
- postprocessing

The details of the first two steps can be referred in COMSOL’s manual [7]. Figure 1 shows the pressure and velocity distribution of the fluid (air) when a cantilever (only the rectangular cross-section is shown) is oscillating horizontally with a sinusoidal velocity. In the postprocessing step, by integrating the stress and pressure around the boundary of the cross-section, the corresponding drag force is also found to be sinusoidal for steady oscillation. Typical simulation results are shown in figure 2. In the figure, both the drag force (per unit length) and the corresponding velocity are plotted. Clearly there is a phase lag (θ) of the drag force compared to the velocity. Generally this phase lag is oscillatory frequency dependent. For small dimensionless frequency λ , the

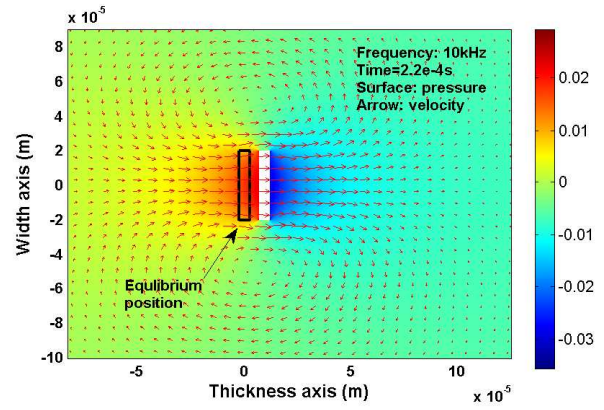


Figure 1: COMSOL simulation of cantilever oscillation ($10kHz$) in air: pressure and velocity of the fluid

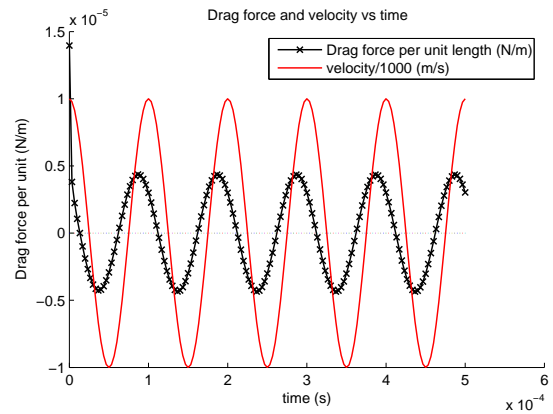


Figure 2: Fluid drag force and the corresponding velocity: phase lag

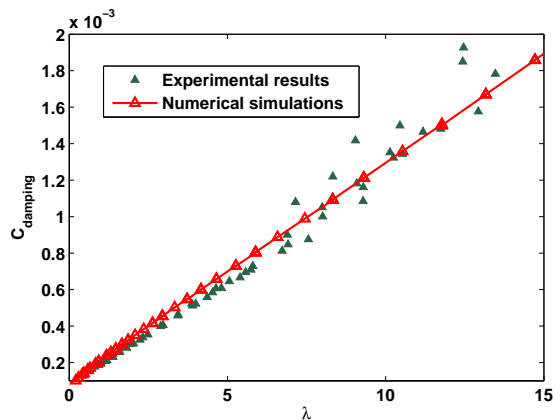


Figure 3: $C_{damping}$: Simulation results and experimental data

drag force is almost in-phase with the velocity ($\theta \approx 0$). But for greater λ , they can be close to 90 degrees out-of-phase ($\theta \approx \frac{\pi}{2}$). In general, the drag force (F) has two components: one is in-phase with the velocity (denoted as F_{\parallel}) and the other is 90 degrees out-of-phase (denoted as F_{\perp}), or

$$F_{\parallel} = F * \cos \theta \quad (3)$$

$$F_{\perp} = F * \sin \theta \quad (4)$$

F_{\parallel} contributes to the fluid damping, while F_{\perp} contributes to the additional ‘‘mass’’ to the cantilever, which will result in an resonant frequency left shift for the resonator.

2.2 Comparison with experiments

The testing method and setup are introduced in [6]. MEMS cantilevers made from single crystal silicon with dimensional variations (widths and thicknesses) are tested at different resonant modes to extract the damping coefficients. The frequency shift attribute of the damping force was below the frequency resolution of the experiment and thus wasn't recorded. Both the experimental results and the numerical simulation results are shown and compared in figure 3 with respect to parameter λ in (2). The good agreement not only validates the numerical analysis, but also it provides a way to extract the parameter pair (a, b) by the curve fitting. For the cantilever, from figure (3), we have $a \approx 1.45$ and $b \approx 2.06$, or

$$C_{damping} \approx (1.45 + 2.06\lambda)\pi\mu \quad (5)$$

3 MODEL GENERALIZATION

3.1 Parameter a and its sensitivity to different cross-sections

The parameter a has a dominant damping influence in (1) for systems with low dimensionless frequency, $\lambda \sim 0$. For the rectangular cross-section resonators such as cantilever, there is no simple analytical expression. However for elliptic cylinder shown in figure 4, Oseen derived an expression of the drag force [8], of which the corresponding a has the following form:

$$a = \frac{4}{\frac{d_1}{d_1+d_2} - \gamma - \log\left(\frac{Re}{16} \frac{d_1+d_2}{d_2}\right)} \quad (6)$$

where γ is the Euler constant and Re is the Reynolds number. Two assumptions are made for (6). First is that the minor axis (d_1) is parallel to the velocity direction, the other is that the Reynolds number (Re) is smaller than 1 which is usually satisfied in micro and nano fluidics. For circular cross-section,

$$a = \frac{4}{0.5 - \gamma - \log\left(\frac{Re}{8}\right)} \quad (7)$$

and for cross-section with high aspect ratio ($d_2 \gg d_1$),

$$a = \frac{4}{-\gamma - \log\left(\frac{Re}{16}\right)} \quad (8)$$

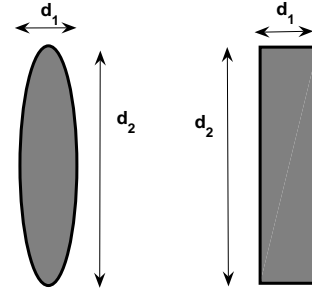


Figure 4: Elliptic and rectangular cross-sections

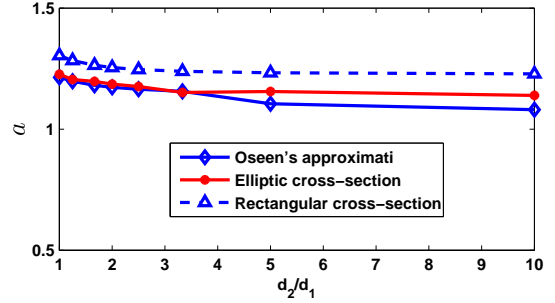


Figure 5: Static damping: Oseen's approximation, numerical simulations

For a rectangular cross-section with high aspect ratio (shown in figure 4), (6) can be used as an approximation. The simulation method introduced before is used to check the error. We compare the difference of parameter a between rectangular and elliptic cross-sections with respect to the aspect ratio d_2/d_1 . The results are plotted in figure 5, from which it can be seen that approximation (6) can be safely used to model the rectangular cross-section case with less than 10% relative error, even when $d_2/d_1 \approx 1$.

All the expressions for parameter a (6-8) are for steady flow. For oscillatory cases, because Reynolds number Re is no longer uniform for the whole device, one must interpolate an average value of a according to the Reynolds number range. Figure 6 shows the plot for expression (8).

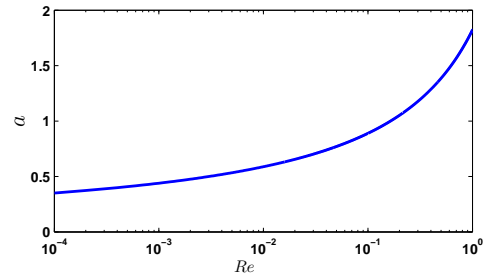


Figure 6: Reynolds number dependent parameter a

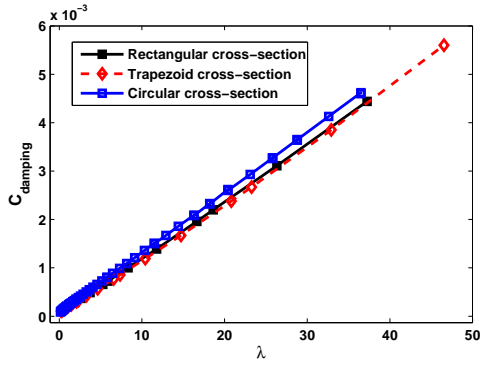


Figure 7: $C_{damping}$ for three types of cross-sections

3.2 Parameter b and its sensitivity to different cross-sections

Determination of parameter b is subjected to numerical analysis and comparison to experimental results. From experimental results displayed in figure 3, parameter b is extracted:

$$b \approx 2 \quad (9)$$

(9) is only for the rectangular cross-section with specific thickness ($5\mu m$ thickness for tested cantilevers). Therefore, to generate (9), there exist two concerns. The first is its sensitivity to differently shaped cross-sections. Due to the fact that damping model (1) ignores the effect of device dimension parallel to the flow, the second concern is the sensitivity of parameter b to this dimension. In our example, this dimension is the thickness (d_1) for the cantilever.

The damping coefficients for the following three different cross-section shapes are compared: rectangular ($5\mu m$ thickness, $100\mu m$ width), trapezoid and circular cross-sections. The results are shown in figure 7, from which it can be shown that the relative differences among are less than 5%. This indicates that parameter b is insensitive to device cross-sectional shape. For cross-section with non-streamlined boundary (such as the rectangular cross-section), the thickness effect can not be ignored when the thickness (d_1) is comparable with the width (d_2). Numerically we compare the damping coefficients for different resonant frequency and width combinations with varying thickness. The results are shown in figure 8, from which it shows that for high width-to-thickness ratio ($d_2/d_1 > 5$), the effect of the thickness is insignificant.

By combining the discussion above about parameters a and b , the linear damping model (1) can be generalized. For the beam-type resonator, the fluid damping can be written as:

$$C_{damping} = (a + 2\lambda)\pi\mu \quad (10)$$

with $< 10\%$ overall error, where parameter a is shown in (6-8). For resonators with non-streamlined cross-sections (examples: rectangular and trapezoid cross-sections), using (10) requires a high aspect-ratio ($d_2/d_1 > 5$) for the cross-section. Furthermore, for high frequency application ($\lambda \gg$

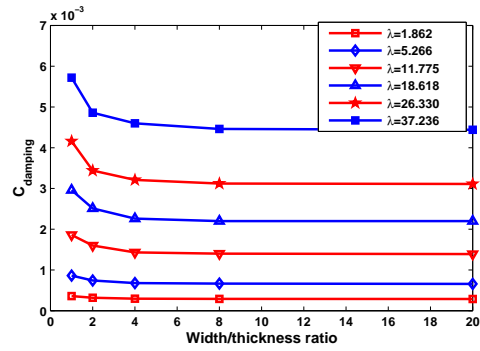


Figure 8: Effect of the thickness to the fluid damping

1), (10) is simply:

$$C_{damping} = 2\lambda\pi\mu \quad (11)$$

4 CONCLUSIONS

This research is aimed to improve Q factor prediction and therefore to improve the design of the flexural oscillation based micro and nano sensors and actuators, which operate in high damping medium such as air and liquid. We quantitatively validate and generalize the frequency and geometry-dependent fluid damping model for MEMS and NEMS flexural resonators with differently shaped cross-sections. By determining the parameter pair (a, b) in (1) and investigating their sensitivities to both the cross-section shape and dimension parallel to the flow, a widely applicable damping law is given in (10) and (11) with limited overall error ($< 10\%$). Although only three types of cross-section are considered in this paper, the sample represents a large constituent of technically relevant flexural oscillators.

REFERENCES

- [1] K.Y. Yasummura et al. "Quality factors in micron and submicron thick cantilevers" J.MEMS V9(1), 2000
- [2] M.K. Ghatkesar, "Real-time mass sensing by nanomechanical resonators in fluid", IEEE Sensors, Vienna, Oct 2004
- [3] W. Zhang and K. L. Turner, "Application of parametric resonance amplification in a single-crystal silicon micro-oscillator based mass sensor", Sensors and Actuators A: Physical, V122, 23-30, 2005
- [4] K. Aihara, J. Xiang, S. Chopra, A. Pham and R. Apprao, "GHz carbon nanotube resonator biosensors", IEEE Nanotechnologies, Nov 2005
- [5] L.D. Landau and E.M. Lifshitz, Fluid Mechanics, 1959
- [6] W. Zhang and K.L. Turner, "Pressure-Dependent Damping Characteristics of Micro Silicon Beam Resonators for Different Resonant Modes", IEEE Sensors, Irvine, Nov 2005
- [7] COMSOL manual and demo
- [8] H. Lamb, Hydrodynamics, 1932